PHYSICAL REVIEW A **94**, 051602(R) (2016)

Finite-temperature hydrodynamics for one-dimensional Bose gases: Breathing-mode oscillations as a case study

I. Bouchoule,[1] S. S. Szigeti,[2,3] M. J. Davis,[2] and K. V. Kheruntsyan[2]

[1]*Laboratoire Charles Fabry, Institut d'Optique, CNRS, Univesité Paris Sud 11, 2 Avenue Augustin Fresnel, F-91127 Palaiseau Cedex, France*

[2]*University of Queensland, School of Mathematics and Physics, Brisbane, Queensland 4072, Australia*

[3]*ARC Centre of Excellence for Engineered Quantum Systems, University of Queensland, Brisbane, Queensland 4072, Australia*

(Received 4 March 2016; published 7 November 2016)

We develop a finite-temperature hydrodynamic approach for a harmonically trapped one-dimensional quasicondensate and apply it to describe the phenomenon of frequency doubling in the breathing-mode oscillations of the quasicondensate momentum distribution. The doubling here refers to the oscillation frequency relative to the oscillations of the real-space density distribution, invoked by a sudden confinement quench. By constructing a nonequilibrium phase diagram that characterizes the regime of frequency doubling and its gradual disappearance, we find that this crossover is governed by the quench strength and the initial temperature rather than by the equilibrium-state crossover from the quasicondensate to the ideal Bose gas regime. The hydrodynamic predictions are supported by the results of numerical simulations based on a finite-temperature c-field approach and extend the utility of the hydrodynamic theory for low-dimensional quantum gases to the description of finite-temperature systems and their dynamics in momentum space.

DOI: 10.1103/PhysRevA.94.051602

Hydrodynamics is a powerful and broadly applicable approach for characterizing the collective nonequilibrium behavior of a wide range of classical and quantum fluids, including Fermi liquids, liquid helium, and ultracold atomic Bose and Fermi gases [1–6]. For ultracold gases, the hydrodynamic approach has been particularly successful in describing the breathing (monopole) and higher-order (multipole) collective oscillations of harmonically trapped three-dimensional (3D) Bose-Einstein condensates [2,6,7]. For condensates near zero temperature, the applicability of the approach stems from the fact that for long-wavelength (low-energy) excitations the hydrodynamic equations are essentially equivalent to those of superfluid hydrodynamics, which in turn can be derived from the Gross-Pitaevskii equation for the order parameter. For partially condensed samples at finite temperatures, the hydrodynamic equations should be generalized to the equations of two-fluid hydrodynamics, where the applicability of the approach to the normal (thermal) component of the gas is justified by fast thermalization times due to collisional relaxation [3,8].

In contrast to 3D systems, the applicability of the hydrodynamic approach to 1D Bose gases is not well established. First, in the thermodynamic limit 1D Bose gases lack the long-range order required for superfluid hydrodynamics to be *a priori* applicable. Second, the very notion of local thermalization, required for the validity of collisional hydrodynamics of normal fluids, is questionable due to the underlying integrability of the uniform 1D Bose gas model [9]. Despite these reservations, the hydrodynamic approach has already been applied to zero-temperature ($T = 0$) dynamics of 1D Bose gases in various scenarios [10–15] (for related experiments, see [16–18]). The comparison of hydrodynamic predictions with exact theoretical results is challenging. In Ref. [13], time-dependent density-matrix renormalization-group simulations of the collision of 1D Bose gases at $T = 0$ found reasonable agreement with the hydrodynamic approximation, although the latter failed to predict short-wavelength dynamics such as shock waves. An alternative approximate approach, based on the conservation of Lieb-Liniger rapidities, has been applied to describe the free-expansion dynamics of a $T = 0$ 1D gas [15] and was able to reproduce the hydrodynamic results for both weak and strong interactions.

At finite temperatures, finding exact predictions is extremely difficult and thus developing a hydrodynamic approach is appealing, despite its lack of justification. Here we develop a general finite-T hydrodynamic approach suitable for 1D Bose gases and specifically apply it to the breathing-mode oscillations of a harmonically trapped 1D quasicondensate. We find that the predictions agree with both experimental observations [18] and numerical simulations of a finite-temperature c-field methodology [19,20]. More remarkably, our hydrodynamic approach not only adequately describes the dynamics of the density distribution of the gas (the standard observable of the hydrodynamic theory), but it can also be used to describe the dynamics of the *momentum distribution*, which is a key observable for quantum gas experiments.

Reference [18] experimentally studied confinement quenches of a finite-T 1D Bose gas. The key finding was the phenomenon of frequency doubling in the oscillations of the momentum distribution relative to the breathing-mode oscillations of the real-space density profile. For the experimental data set deep in the quasicondensate regime, a periodic narrowing of the momentum distribution occurred at twice the frequency of the breathing mode of the density profile. Although finite-temperature effects are crucial for understanding the momentum-space properties of *equilibrium* quasicondensates [21–26], the said experimental data for *dynamics* were well described by a simple zero-temperature classical hydrodynamic approach, wherein the frequency doubling was interpreted as a result of a self-reflection mechanism due to the mean-field interaction energy barrier. In contrast to this behavior, no frequency doubling was observed in the nearly ideal Bose gas regime, as expected for a noninteracting gas. A theoretical explanation for the experimentally observed

smooth crossover from the regime of frequency doubling to no doubling is lacking.

Here we explain this phenomenon within the hydrodynamic approach and construct the corresponding nonequilibrium phase diagram, showing that the frequency-doubling crossover is governed by the quench strength and a nontrivial combination of the temperature and interaction strength. For small enough quenches, the crossover from frequency doubling to no doubling can lie entirely within the quasicondensate regime and does not require an equilibrium-state crossover to the ideal Bose gas regime. Constructing and studying phase diagrams is an important goal in many areas of physics and our findings here serve as an example where equilibrium and dynamical phase diagrams are not identical. We confirm our predictions by comparing the hydrodynamic results to those obtained numerically using finite-temperature c-field simulations (for a review, see [20]) based on the projected Gross-Pitaevskii equation [19].

(a) Hydrodynamic equations and evolution of the density distribution. The hydrodynamic approach relies on the local-density approximation and assumes that the 1D system can be divided into small locally uniform slices, each of which is in thermal equilibrium in the local moving frame. Moreover, one can assume that heat transfer between the slices is negligible for long-wavelength excitations [27], which implies that each slice undergoes isentropic decompression or compression. The hydrodynamic description of this system is [1]

$$\partial_t \rho + \partial_x(\rho v) = 0, \tag{1a}$$

$$\partial_t v + v\partial_x v = -\frac{1}{m}\partial_x V(x,t) - \frac{1}{m\rho}\partial_x P, \tag{1b}$$

$$\partial_t s + v\partial_x s = 0, \tag{1c}$$

where $\rho(x,t)$ is the local 1D density of the slice at position x, $v(x,t)$ is the respective hydrodynamic velocity, $s(x,t)$ is the entropy per particle, $P(x,t)$ is the pressure, m is the mass of the constituent particles, and $V(x,t)$ is the external trapping potential, which for our case study is harmonic, $V(x,t) = \frac{1}{2}m\omega(t)^2x^2$, of frequency $\omega(t)$.

We now apply the hydrodynamic approach to describe the postquench dynamics induced by the following scenario. Initially, the atomic cloud with density profile $\rho_0(x)$ is in thermal equilibrium at temperature T_0 in the trap of frequency ω_0. Subsequently, at time $t = 0$, the trap frequency is suddenly changed to ω_1. To characterize the ensuing dynamics in different regimes of the 1D Bose gas, we introduce the dimensionless interaction parameter $\gamma_0 = mg/\hbar^2\rho_0(0)$ and the dimensionless temperature $t_0 = 2\hbar^2k_BT_0/mg^2$ [28,29], where g is the coupling strength of the pairwise δ-function interaction potential. The solutions of the hydrodynamic equations (1a)–(1c) describing this harmonic-confinement quench depend only on the thermodynamic equation of state of the gas. In each of the following three cases, (i) the ideal gas regime ($t_0,\gamma_0^{3/2}t_0 \gg 1$), (ii) the strongly interacting or Tonks-Girardeau regime ($\gamma_0, 1/t_0 \gg 1$), and (iii) the quasicondensate regime ($\gamma_0,\gamma_0^{3/2}t_0 \ll 1$), the solutions reduce to scaling equations of the form

$$\rho(x,t) = \rho_0[x/\lambda(t)]/\lambda(t), \quad v(x,t) = x\dot{\lambda}(t)/\lambda(t), \tag{2}$$

$$T(t) = T_0/\lambda(t)^{\nu+1}, \tag{3}$$

where the scaling parameter $\lambda(t)$ [with $\dot{\lambda} \equiv d\lambda(t)/dt$, $\lambda(0) = 1$, and $\dot{\lambda}(0) = 0$] satisfies the ordinary differential equation

$$\ddot{\lambda} = -\omega_1^2\lambda + \omega_0^2/\lambda^{2\nu+1}, \tag{4}$$

with the value of ν in different regimes given below [30]. The hydrodynamic solution (3) for the temperature is one of the key results of this paper as it allows one to simply calculate the evolution of the temperature-dependent momentum distribution of the gas (see below).

(i) Ideal gas regime ($t_0,\gamma_0^{3/2}t_0 \gg 1$). In this case $\nu = 1$ and the validity of the above scaling solutions can be demonstrated using a dimensional analysis of the equation of state (see Ref. [31]), which we note is also applicable to an ideal Fermi gas. Equation (4) in this regime has an explicit analytic solution

$$\lambda(t) = \sqrt{1 + \epsilon\sin^2(\omega_1 t)}. \tag{5}$$

This corresponds to harmonic oscillations of the mean-square width of the density profile, occurring at frequency $\omega_B = 2\omega_1$, with $\epsilon \equiv (\omega_0/\omega_1)^2 - 1$ characterizing the quench strength. This result coincides with that for a noninteracting gas obtained from a single-particle picture. The fact that the hydrodynamic approach, which *a priori* assumes sufficient collisions to ensure local thermal equilibrium, agrees with the results for a noninteracting gas is specific to the harmonic-confinement quench considered here and is accidental.

(ii) Strongly interacting regime ($\gamma_0, 1/t_0 \gg 1$). Here the equation of state is that of an ideal Fermi gas, so the previous ideal gas results apply and Eqs. (2)–(4) are fulfilled with $\nu = 1$. The breathing-mode oscillations of the momentum distribution of a finite-temperature Tonks-Girardeau gas are discussed elsewhere [32].

(iii) Quasicondensate regime ($\gamma_0,\gamma_0^{3/2}t_0 \ll 1$). In this case $\nu = 1/2$ and the validity of the scaling solutions (2) can be demonstrated using the equation of state $P = \frac{1}{2}g\rho^2$. The latter can be derived from the quasicondensate chemical potential $\mu = g\rho$ and the Gibbs-Duhem relation $\rho = (\partial P/\partial\mu)_T$. For a weak quench $\epsilon \ll 1$, the solution to Eq. (4) oscillates at frequency $\omega_B \simeq \sqrt{3}\omega_1$ and is nearly harmonic with an amplitude $\lambda(t = \pi/\omega_B) - 1 \simeq 2\epsilon/3$ [33]. According to Eq. (2), the density profile breathes self-similarly, maintaining its initial Thomas-Fermi parabolic shape, $\rho_0(x) = \rho_0(0)(1 - x^2/X_0^2)$ for $x \leqslant X_0$ [$\rho_0(x) = 0$ otherwise], with $X_0 = \sqrt{2g\rho_0(0)/m\omega_0^2}$. Finite-temperature effects are not seen in the dynamics of the density distribution $\rho(x,t)$ [34] because in this regime the equation of state does not depend on the temperature. However, as we show below, such effects can be revealed in the dynamics of the momentum distribution.

(b) Dynamics of the momentum distribution. Let us consider a slice of the gas in the region $[x, x + dx]$ of density $\rho(x,t)$, velocity $v(x,t)$, and entropy per particle $s(x,t)$. In the laboratory frame its momentum distribution is $\overline{n}(\rho,s,k - mv/\hbar)$, where $\overline{n}$ is the equilibrium momentum distribution of a homogeneous gas, which we normalize to $\int dk\,\overline{n}(\rho,s;k) = \rho$. The total momentum distribution is then given by

$$n(k,t) = \int dx\,\overline{n}(\rho,s;k - mv(x,t)/\hbar). \tag{6}$$

There are two contributions to $n(k,t)$, the hydrodynamic velocity field and the contribution of thermal velocities, which have different effects on the breathing-mode oscillations. In order to see the sole effect of the hydrodynamic velocity field, let us first disregard the effect of the thermal velocities, taking $\overline{n}(\rho,s;k-mv(x,t)/\hbar)=\rho\delta(k-mv(x,t)/\hbar)$, where $\delta(k)$ is the Dirac delta function. If a scaling solution as in Eq. (2) exists, the hydrodynamic component of the momentum distribution evolves according to

$$n_{\rm h}(k,t)=\frac{\hbar}{m|\dot{\lambda}|}\rho_0\left(\frac{\hbar k}{m\dot{\lambda}}\right). \tag{7}$$

For oscillatory $\lambda(t)$, this implies that $n_{\rm h}(k,t)$ collapses to a zero-width distribution *twice* per position-space density breathing cycle: when the width of the cloud in real space is both largest and smallest, both corresponding to $\dot{\lambda}=0$. Therefore, the oscillations of the hydrodynamic contribution to the momentum distribution will always display frequency doubling.

Now consider the additional contribution of thermal velocities to $n(k,t)$, which changes as each slice undergoes isentropic compression and decompression during the breathing cycle. Since one expects the momentum width to be a monotonically increasing function of the compression factor, the thermal momentum width of each slice [and hence of the overall momentum distribution $n(k,t)$] is expected to oscillate out of phase relative to the width of the real-space density profile, but at the same breathing frequency ω_B.

The evolution of the overall momentum distribution $n(k,t)$ results from the combination of the hydrodynamic and thermal parts. For a near-ideal gas at $T>0$ this leads to a somewhat fortuitous cancellation of the hydrodynamic velocity field by the thermal component and so the total momentum distribution always oscillates at $\omega_B=2\omega_1$ (see Ref. [31]) and never displays frequency doubling, consistent with the single-particle picture.

The situation is different, however, in the quasicondensate regime. The momentum distribution of a homogeneous quasicondensate of density ρ and temperature T, for wavelengths in the phononic regime (i.e., $k\ll\hbar/\sqrt{mg\rho}$), is given by a Lorentzian $\overline{n}(\rho,s;k)=(2\rho l_\phi/\pi)/[1+(2l_\phi k)^2]$ [31]. Substituting this Lorentzian into Eq. (6), we obtain the full momentum distribution of the trapped gas

$$n(k,t)=\frac{1}{\pi}\int dx\,\frac{2l_\phi(x,t)\rho(x,t)}{1+4[l_\phi(x,t)]^2[k-mv(x,t)/\hbar]^2}, \tag{8}$$

where $l_\phi(x,t)=\hbar^2\rho(x,t)/mk_BT(t)$. According to the scaling solutions (2) and (3) with $\nu=1/2$ (see also [31]), $l_\phi(x,t)$ evolves as

$$l_\phi(x,t)=\sqrt{\lambda}l_\phi^{(0)}\tilde{\rho}_0(x/\lambda), \tag{9}$$

where $\tilde{\rho}_0(x)=1-x^2/X_0^2$ is the scaled initial density profile and $l_\phi^{(0)}=\hbar^2\rho_0(0)/mk_BT_0=2[\rho_0(0)\gamma_0^2t_0]^{-1}$.

Combining the scaling solution for $l_\phi(x,t)$ with that for $\rho(x,t)$ and changing variables to $u=x/\lambda X_0$ in Eq. (8) leads to the final result

$$n(k,t)=B\sqrt{\tilde{\lambda}}\int_{-1}^{1}du\,\frac{(1-u^2)^2}{1+4\tilde{\lambda}(1-u^2)^2\left(\tilde{k}-\frac{\omega_1}{\omega_0}A\dot{\tilde{\lambda}}u\right)^2}. \tag{10}$$

Here $\tilde{k}=l_\phi^{(0)}k$, $A=m\omega_0X_0l_\phi^{(0)}/\hbar=\sqrt{8}/\gamma_0^{3/2}t_0$, and $B=2\rho_0(0)l_\phi^{(0)}X_0/\pi$ is a normalization factor. In addition, we have introduced a dimensionless time $\tau\equiv\omega_1t$, so the dimensionless functions $\tilde{\lambda}(\tau)\equiv\lambda(\tau/\omega_1)$ and $\dot{\tilde{\lambda}}=d\tilde{\lambda}/d\tau$, obtained from Eq. (4), depend only on the ratio ω_1/ω_0 or, equivalently, only on the quench strength $\epsilon=(\omega_0/\omega_1)^2-1$. Thus, for a given ϵ, the evolution of $n(k,t)$ is governed solely by the dimensionless parameter A, which itself depends only on the initial intensive parameters γ_0 and t_0. Note that $A\gg1$ in the quasicondensate regime where $\gamma_0^{3/2}t_0\ll1$ [25,28].

Using Eq. (10) for a given A and quench strength ϵ, we can now compute the evolution of the full momentum distribution and its half-width at half maximum (HWHM) [see Figs. 1(a) and 1(b)]. The HWHM can then be fitted with a sum of two sinusoidal functions: the fundamental mode oscillating at ω_B ($\simeq\sqrt{3}\omega_1$, for $\epsilon\ll1$) and the first harmonic oscillating at $2\omega_B$, with amplitudes c_1 and c_2, respectively. Defining the weight of the fundamental mode as $K=c_1^2/(c_1^2+c_2^2)$, we identify the frequency-doubling phenomenon with $K\ll1$, whereas $K\simeq1$ corresponds to the absence of doubling. The doubling crossover can therefore be defined as the value of $A=A_{\rm cr}$ for which $K=1/2$. As we show in [31], for small quench amplitudes one expects the frequency doubling to occur for $A\sqrt{\epsilon}\gg1$, while for $A\sqrt{\epsilon}\ll1$ the thermal effects dominate and the frequency doubling is absent; accordingly, $A_{\rm cr}$ is expected to scale as $A_{\rm cr}\propto1/\sqrt{\epsilon}$. Figure 1(c) shows the nonequilibrium phase diagram of the crossover from frequency doubling to no doubling and confirms that $A_{\rm cr}$, obtained using Eq. (10) and the fitting procedure described above, does indeed scale proportionally to $1/\sqrt{\epsilon}$.

In Fig. 1(d) we superimpose the conditions for observing frequency doubling on the equilibrium phase diagram of the 1D Bose gas. As we see, for small enough quench strengths, the crossover from doubling to no doubling lies well within the quasicondensate regime. We therefore conclude that this phenomenon is governed not by the crossover from the ideal Bose gas regime into the quasicondensate regime, but by the competition between the hydrodynamic velocity (which always displays doubling) and the narrowing and broadening of the thermal component of the gas due to adiabatic compression/decompression (which always oscillates at the fundamental frequency ω_B).

Although the applicability of the hydrodynamic theory in this system might be questionable, our analytic results have been benchmarked against finite-temperature c-field simulations (performed using the software package XMDS2 [36]), whose validity for degenerate weakly interacting Bose gases is well established [19,20,37–39]. In this approach, the Bose gas is approximated as a classical field, whose evolution is governed by the time-dependent Gross-Pitaevskii equation, with the initial state being sampled from the classical Gibbs ensemble for the given temperature and density [31]. Qualitatively, the same behavior as in Figs. 1(a) and 1(b) based on the hydrodynamic approach occurs in our c-field simulations [35]; quantitatively, the crossover from doubling to no doubling is in broad agreement with the analytic predictions [see Fig. 1(c)]. Moreover, as we argue in Ref. [31], for sufficiently weak confinement (small ω_0), the c-field dynamics are governed by just two dimensionless parameters

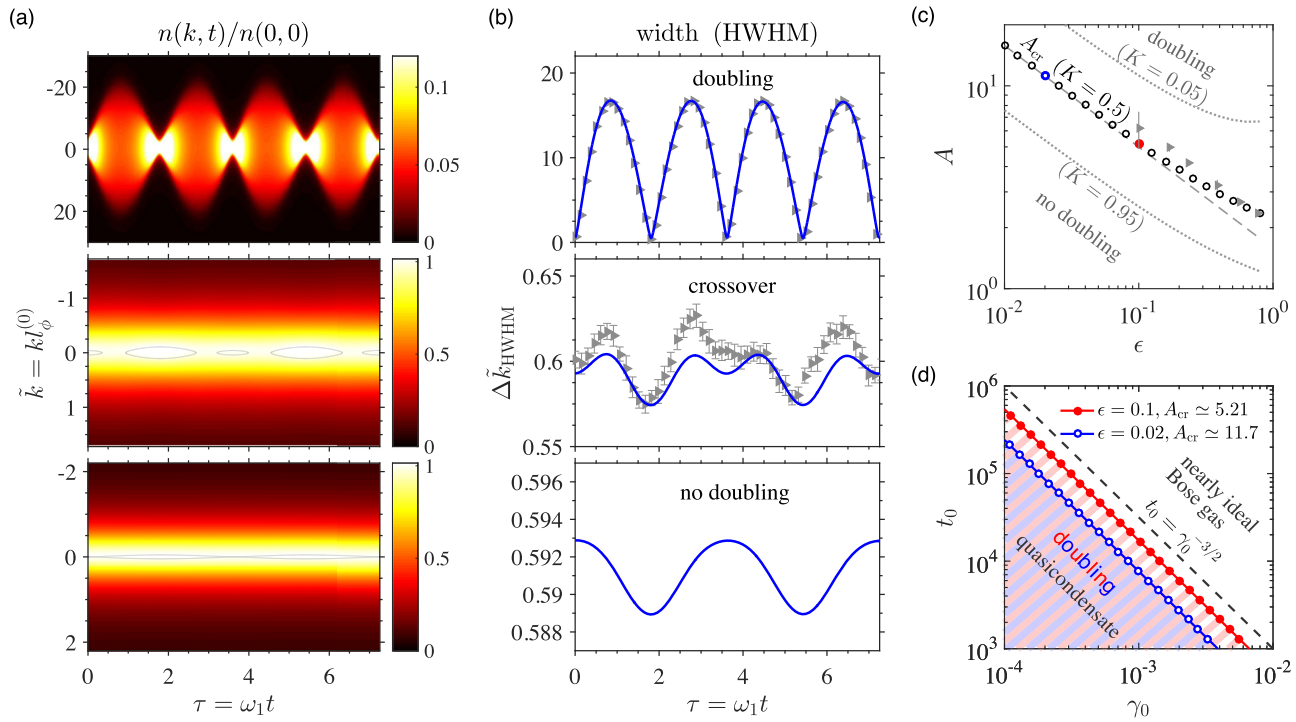

FIG. 1. (a) Breathing-mode oscillations and (b) the respective widths (HWHM) of the momentum distribution of a harmonically trapped 1D quasicondensate after a confinement quench as a function of the dimensionless time $\tau = \omega_1 t$. The three examples shown in (a) and (b) correspond, respectively, to $\epsilon = 0.563$ and $A = 104$ (with $t_0 = 10^6$ and $\hbar\omega_0/g\rho_0(0) = 3.0 \times 10^{-3}$ for the c-field simulations) (top row), $\epsilon = 0.101$ and $A = A_{\rm cr} = 5.21$ ($t_0 = 10^3$ and $\hbar\omega_0/g\rho_0(0) = 1.1 \times 10^{-2}$) (middle row), and $\epsilon = 0.0203$ and $A = 3.95$ (bottom row) [35]. The gray triangles are the c-field data [31], with the error bars indicating a 95% confidence interval. (c) Nonequilibrium phase diagram of the dynamical crossover from frequency doubling to no doubling in the A-ϵ parameter space. Data points (circles) show the crossover values $A_{\rm cr}$ for which the weights of the fundamental and the first harmonics are equal ($K = 1/2$); gray triangles are from c-field simulations. The dashed line is a fit in the region $A > 5$ with a power law $A_{\rm cr} \simeq 1.58/\sqrt{\epsilon}$ (see the text), whereas the two dotted lines show the values of A corresponding to $K = 0.05$ and $K = 0.95$. (d) Frequency-doubling conditions superimposed on the equilibrium phase diagram of the 1D Bose gas [25,28], drawn in terms of the dimensionless temperature t_0 and interaction strength γ_0, and covering the quasicondensate and the neighboring nearly ideal Bose gas regimes. The gray dashed line ($t_0 = \gamma_0^{-3/2}$) corresponds to the crossover between the two equilibrium regimes. The two lines with closed (red) and open (blue) circles, on the other hand, correspond to the frequency-doubling crossover conditions for two different quenches $\epsilon = 0.1$ and $\epsilon = 0.02$ [the respective data points in (c) are labeled in the same way]. The (light red and light blue) shaded areas underneath these lines correspond to the conditions where the frequency doubling occurs.

A and ϵ, as predicted from the hydrodynamic approach. Overall, the performance of the hydrodynamic theory, as validated by our c-field simulations, in modeling the harmonic confinement quench of a finite-temperature quasicondensate is remarkable. Moreover, even though the hydrodynamic results of Eq. (10) formally require $A \gg 1$ to ensure the applicability of the quasicondensate regime, our comparison with c-field simulations shows that Eq. (10) continues to give accurate predictions even for moderate values of $A \gtrsim 1$.

In summary, we have developed a finite-temperature hydrodynamic approach for a harmonically trapped 1D Bose gas and applied it to the study of breathing mode oscillations in the quasicondensate regime. While the usual scope of the hydrodynamic theory is to describe the evolution of the real-space density of a gas, our approach extends its utility to describe the evolution of its momentum distribution. The approach allowed us to discern the contribution of the hydrodynamic velocity field and that of thermal excitations in the oscillatory dynamics of the momentum distribution of the 1D quasicondensate, hence explaining the full mechanism behind the phenomenon of frequency doubling and the crossover to no doubling. The hydrodynamic predictions are in broad agreement with numerical simulations based on finite-temperature c-field simulations. Our approach can address not only the sudden quench scenario studied here, but also the dynamics under arbitrary driving of the trapping frequency $\omega(t)$, in which case the differential equation for the scaling parameter $\lambda(t)$, Eq. (4), must be solved numerically. Future extensions of this work will concern the treatment of breathing-mode oscillations in the strongly interacting regime [32] and could also address collective behavior of 1D Bose gases in anharmonic traps, as well as of 2D and 3D quasicondensates in highly elongated geometries.

K.V.K. acknowledges stimulating discussions with D. M. Gangardt. I.B. acknowledges support from the Centre de Compétences Nanosciences Île-de-France, S.S.S. acknowledges support from the Australian Research Council Centre of Excellence for Engineered Quantum Systems (Grant No. CE110001013), and M.J.D. and K.V.K. acknowledge support from the ARC Discovery Project Grants No. DP160103311

and No. DP140101763. Numerical simulations were run on the University of Queensland School of Mathematics and Physics computer "Obelix," with thanks to I. Mortimer for computing support.

[1] L. D. Landau and E. M. Lifshitz, *Fluid Mechanics: Course of Theoretical Physics*, 2nd edition (Pergamon, Oxford, 1987), Vol. 6.

[2] L. P. Pitaevskii and S. Stringari, *Bose-Einstein Condensation* (Clarendon, Oxford, 2003).

[3] A. Griffin, T. Nikuni, and E. Zaremba, *Bose-Condensed Gases at Finite Temperatures* (Cambridge University Press, Cambridge, 2009).

[4] A. Griffin, W.-C. Wu, and S. Stringari, Phys. Rev. Lett. **78**, 1838 (1997).

[5] Y. Kagan, E. L. Surkov, and G. V. Shlyapnikov, Phys. Rev. A **55**, R18 (1997).

[6] L. Pitaevskii and S. Stringari, Phys. Rev. Lett. **81**, 4541 (1998).

[7] S. Stringari, Phys. Rev. Lett. **77**, 2360 (1996).

[8] L. A. Sidorenkov, M. K. Tey, R. Grimm, Y.-H. Hou, L. Pitaevskii, and S. Stringari, Nature (London) **498**, 78 (2013).

[9] E. H. Lieb and W. Liniger, Phys. Rev. **130**, 1605 (1963).

[10] A. Minguzzi, P. Vignolo, M. L. Chiofalo, and M. P. Tosi, Phys. Rev. A **64**, 033605 (2001).

[11] C. Menotti and S. Stringari, Phys. Rev. A **66**, 043610 (2002).

[12] P. Öhberg and L. Santos, Phys. Rev. Lett. **89**, 240402 (2002); P. Pedri, L. Santos, P. Öhberg, and S. Stringari, Phys. Rev. A **68**, 043601 (2003).

[13] S. Peotta and M. Di Ventra, Phys. Rev. A **89**, 013621 (2014).

[14] S. Choi, V. Dunjko, Z. D. Zhang, and M. Olshanii, Phys. Rev. Lett. **115**, 115302 (2015).

[15] A. S. Campbell, D. M. Gangardt, and K. V. Kheruntsyan, Phys. Rev. Lett. **114**, 125302 (2015).

[16] H. Moritz, T. Stöferle, M. Köhl, and T. Esslinger, Phys. Rev. Lett. **91**, 250402 (2003).

[17] E. Haller, M. Gustavsson, M. J. Mark, J. G. Danzl, G. P. R. Hart, and H.-C. Nägerl, Science **325**, 1224 (2009).

[18] B. Fang, G. Carleo, A. Johnson, and I. Bouchoule, Phys. Rev. Lett. **113**, 035301 (2014).

[19] M. J. Davis, S. A. Morgan, and K. Burnett, Phys. Rev. Lett. **87**, 160402 (2001).

[20] P. B. Blakie, A. S. Bradley, M. J. Davis, R. J. Ballagh, and C. W. Gardiner, Adv. Phys. **57**, 363 (2008).

[21] D. S. Petrov, G. V. Shlyapnikov, and J. T. M. Walraven, Phys. Rev. Lett. **85**, 3745 (2000).

[22] S. Richard, F. Gerbier, J. H. Thywissen, M. Hugbart, P. Bouyer, and A. Aspect, Phys. Rev. Lett. **91**, 010405 (2003).

[23] A. H. van Amerongen, J. J. P. van Es, P. Wicke, K. V. Kheruntsyan, and N. J. van Druten, Phys. Rev. Lett. **100**, 090402 (2008).

[24] S. Hofferberth, I. Lesanovsky, B. Fischer, T. Schumm, and J. Schmiedmayer, Nature (London) **449**, 324 (2007).

[25] T. Jacqmin, J. Armijo, T. Berrada, K. V. Kheruntsyan, and I. Bouchoule, Phys. Rev. Lett. **106**, 230405 (2011).

[26] J. Armijo, T. Jacqmin, K. Kheruntsyan, and I. Bouchoule, Phys. Rev. A **83**, 021605 (2011).

[27] As is well known in acoustic physics, the contribution of heat transfer, estimated using a diffusion equation, to local changes of the energy per particle is negligible for long-wavelength deformations.

[28] K. V. Kheruntsyan, D. M. Gangardt, P. D. Drummond, and G. V. Shlyapnikov, Phys. Rev. A **71**, 053615 (2005).

[29] I. Bouchoule, K. V. Kheruntsyan, and G. V. Shlyapnikov, Phys. Rev. A **75**, 031606 (2007).

[30] We note that Eq. (4) and the scaling solutions (2) and (3) remain applicable for arbitrary time variation of $\omega_1(t)$.

[31] See Supplemental Material at http://link.aps.org/supplemental/10.1103/PhysRevA.94.051602, for additional proofs and clarifications of various aspects of the hydrodynamic solutions, as well as the details of c-field simulations.

[32] Y. Atas, I. Bouchoule, D. M. Gangardt, and K. V. Kheruntsyan, arXiv:1608.08720.

[33] For a small-amplitude quench ($\epsilon \ll 1$), Eq. (4) with $\nu = 1/2$ can be solved using the method of linearization [i.e., expanding $\lambda(t)$ as $\lambda(t) = 1 + \delta\lambda(t)$, with $\delta\lambda(t) \ll \lambda(t)$], yielding $\lambda(t) \simeq 1 + \frac{\epsilon}{3} - \frac{\epsilon}{3}\cos(\sqrt{3}\omega_1 t)$.

[34] According to the quasicondensate equation of state, the last term in the hydrodynamic equation (1b), $\frac{1}{\rho}\partial_x P = g\partial_x \rho$, does not depend on temperature T and is in fact the same as for a $T = 0$ gas. Therefore, the hydrodynamic equations for the density and velocity fields decouple from the equation for s and consequently no finite-temperature effects are seen in the dynamics of $\rho(x,t)$ and $v(x,t)$.

[35] The regime of no doubling [bottom row in Figs. 1(a) and 1(b)], corresponding to a very small quench strength, is inaccessible in the c-field method due to large sampling errors.

[36] G. R. Dennis, J. J. Hope, and M. T. Johnsson, Comput. Phys. Commun. **184**, 201 (2013).

[37] M. J. Davis, P. B. Blakie, A. H. van Amerongen, N. J. van Druten, and K. V. Kheruntsyan, Phys. Rev. A **85**, 031604 (2012).

[38] A. Sinatra, Y. Castin, and C. Lobo, J. Mod. Opt. **47**, 2629 (2000).

[39] Y. Castin, R. Dum, E. Mandonnet, A. Minguzzi, and I. Carusotto, J. Mod. Opt. **47**, 2671 (2000).